Starting Structure Dependence of NMR Order Parameters Derived from MD Simulations: Implications for Judging Force-Field Quality

Alrun N. Koller,* Harald Schwalbe,[†] and Holger Gohlke*

*Department of Biological Sciences, [†]Department of Biochemistry, Chemistry, and Pharmacy, Institute for Organic Chemistry and Chemical Biology, Center for Biomolecular Magnetic Resonance, Goethe-University, Frankfurt am Main, Germany

ABSTRACT   Comparing experimental generalized N-H S^2 order parameters to those calculated from molecular dynamics trajectories is increasingly used to judge force-field quality and completeness of sampling. Herein we demonstrate for the well-investigated system hen egg white lysozyme that different experimental starting structures can lead to significant differences in molecular-dynamics-derived S^2 parameters that can be even larger than S^2 parameter deviations due to different force fields. Caution should thus be taken in general when simulated S^2 parameters are compared to experimental data with the aim of judging force-field quality. We show that adequately sampling flexible regions ($\sim$100 ns) and only calculating S^2 parameters averaged over short time windows proved necessary to obtain consistent results irrespective of the starting structure.

Molecular dynamics (MD) simulations and NMR spin relaxation spectroscopy are complementary tools to investigate the dynamics of biomolecules (1,2). Comparing experimental NMR spin relaxation data to those calculated from MD trajectories also allows assessing whether MD simulations accurately reproduce structural and dynamical properties of the system (3). A comparison of experimental and MD-derived N-H S^2 order parameters (4) is increasingly used to judge force-field quality in this regard (5–8).

Aside from simulation conditions (5) and the approach used to extract S^2 parameters (9), an influence of the MD starting structure on the computed S^2 parameters ought to be expected too (10,11), considering that system dynamics and (local) structure are intimately related (12). This influence should become particularly pronounced in flexible parts of the molecule, where conformational variability in experimental structures is most likely to occur. Herein, we demonstrate for hen egg white lysozyme (HEWL) that different starting structures can lead to differences in MD-derived S^2 parameters that can be larger than deviations due to different force fields. Accordingly, caution should be taken when simulated S^2 parameters are compared to experimental data with the aim of judging force-field quality.

HEWL is a well-investigated model system that has become a standard for evaluating the quality of force fields in terms of internal dynamics (6–8,13). For investigating a starting structure dependence on calculated S^2 values, we first clustered 92 unbound wild-type HEWL crystal structures with a resolution <2.0 Å and 50 conformations of an NMR ensemble (14) with respect to backbone torsion angles of residues Gly[71] and Asn[74] in the loop 2 region (residues 65–75). The conformations are characterized by the backbone N-H bonds of the two residues either pointing to the protein or to

the solvent, revealing in total four major loop 2 conformations (cluster 1: 32 NMR structures, 37 crystal structures; cluster 2 and 4: 48 and 7 crystal structures; cluster 3: 18 NMR structures) (see Table S1 and Fig. S1 in Supplementary Material, Data S1). Of the three clusters containing crystals structures, we chose one crystal structure each as a starting structure (Fig. 1 a). All three structures have been crystallized in the same space group. Visual inspection of the crystal packings did not reveal any differences in stabilizing interactions by the crystal environment involving the loop 2 region. Hence, we believe that the conformational variance of loop 2 cannot be attributed to differences in crystal packing. For reasons of comparison, we also considered the first model of the NMR ensemble 1E8L (cluster 1).

For each structure we performed MD simulations with periodic boundary conditions in the NVT ensemble using the TIP3P water model at 300 K for a minimum of 30 ns with AMBER9 (15) and applying the ff99 (16) and ff99SB (6) force fields. The MD simulations of 1HEL were extended to 100 ns. S^2 parameters were calculated for backbone N-H bonds according to the isotropic reorientational eigenmode dynamics approach (17). Using an alternative approach applied by Hornak et al. (6) did not result in qualitatively different S^2 values (see Fig. S8 in Data S1).

Initially, we analyzed the structural stability of loop 2 in terms of backbone dihedral angle changes for residues Gly[71] and Asn[74] (see Figs. S2–S5 in Data S1). The backbone dihedrals allow assigning each conformation from the MD simulations to one of the four clusters. With respect to loop
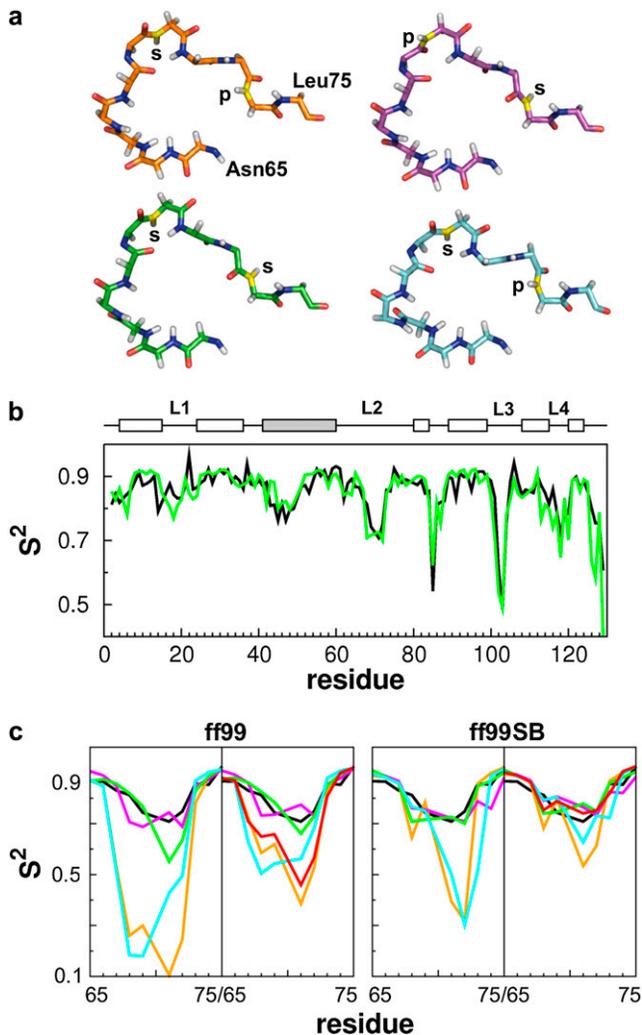
FIGURE 1 (*a*) Residues 65–75 (loop 2) of the investigated HEWL structures (1HEL (*orange*, cluster 1); 1E8L model 1 (*cyan*, cluster 1); 1IEE (*green*, cluster 2); and 6LYT (*magenta*, cluster 4)). The N atoms of Gly[71] and Asn[74] are colored in yellow. Additionally, it is indicated if the N-H bond points to the protein (*p*) or to the solvent (*s*). (*b*) Experimental S^2 values (18) (*black*) are compared to calculated values (*green*) from the 30 ns simulation of 1IEE with ff99SB. Secondary structure elements are indicated by boxes (*white*, helix; *gray*, β-sheet). (*c*) Comparison of experimental (18) (*black*) and calculated S^2 values (colored as in *a*) of loop 2 using ff99 and ff99SB. The S^2 values were either calculated over the whole 30 ns trajectory (*left panels*) or averaged over time windows of 1 ns length (*right panels*). The red line depicts 1 ns time window-averaged S^2 values of 1HEL over 100 ns.

2, the trajectories originating from different starting structures revealed very different structural stabilities (Fig. S6 in Data S1). 6LYT and 1IEE almost exclusively exist in a loop 2 conformation similar to that of cluster 2, with 1IEE showing occasional transitions to the cluster 4 conformation in the case of ff99. In contrast, 1HEL and 1E8L display conformations that resemble those of cluster 1 and 3. Frequent exchanges between these two conformations occur in the case of ff99, but a more restricted loop 2 dynamics is

observed in the case of ff99SB. In no case, transitions between cluster sets {1, 3} and {2, 4} are observed. As we believe that the observed clusters are not due to differences in the energetics of the crystal environments, this points to a poor sampling of the backbone dihedral angle transitions of the peptide bond between Arg[73] and Asn[74]. From the observed differences in the structural stabilities, one can already anticipate computed S^2 parameters of loop 2 to be different across the trajectories due to varying internal dynamics of that region.

Fig. 1 and Fig. S7 in Data S1 show calculated S^2 parameters for the four different starting structures. In all cases, S^2 parameters of ordered regions agree across the different simulations as well as with experiment (18) (RMSD < 0.085; Table S2), irrespective of the force field used (Fig. S7 in Data S1). This observation is in line with previously reported characteristics of the two force fields (5). In contrast, major differences occur in the loop regions of HEWL (residues 16–23, 65–75, 100–107, and 116–119) (Fig. 1, and Fig. S7 in Data S1) and are most pronounced for the loop 2 region. This is not unexpected (6) if different force fields are applied to generate trajectories originating from the same structure (as in the case of 1IEE, Fig. 1 *c*). However, it is disturbing that even larger S^2 differences are observed if trajectories were generated from different structures, but using the same force field (Fig. 1 *c*). In our case, this holds true for both force fields tested. A better agreement between computed and experimental S^2 for the loop 2 region of 6LYT has been found for ff99SB compared to ff99 by Hornak et al. (6), in agreement with similar findings on ubiquitin (5). In contrast, in our case, both ff99 and ff99SB result in S^2 parameters for 6LYT that very well agree with experiment (RMSD = 0.047; 0.048). Similarly, a very good agreement is found for 1IEE with ff99 and ff99SB (RMSD = 0.064; 0.042). In contrast, 1HEL and 1E8L lead to too low S^2 parameters irrespective of the force field used (RMSD > 0.175). These results demonstrate that depending on the initial loop conformation significant differences in computed S^2 parameters are observed, if the whole trajectory is considered at once as done previously (5,6). Obviously, an agreement between computed and experimental S^2 values should be considered fortuitous in this case.

If a simulation exceeds in length the overall tumbling correlation time, S^2 parameters computed over the whole trajectory can include motions that would not be reflected in the experimental S^2 values, leading to a bias in the computed S^2 values (5,19). Thus, we also computed S^2 parameters from the MD simulations after the isotropic reorientational eigenmode dynamics approach (17) for time windows of 1–5 ns in 1 ns steps. The S^2 parameters were subsequently averaged over all available time windows. No qualitative change of S^2 parameters was observed for 6LYT and 1IEE. However, in the case of 1HEL and 1E8L, increased S^2 parameters were found for the loop 2 region for both the ff99 and ff99SB case, with the 1 ns S^2 parameters providing the best results

(RMSD = 0.058–0.153; Table S3 in Data S1), as also found recently (5,19). S^2 parameters computed from the ff99SB trajectories now much better agree with experiment (RMSD = 0.085 (1HEL); 0.058 (1E8L)) than those from the ff99 trajectories (RMSD = 0.153 (1HEL); 0.143 (1E8L)). Encouragingly, S^2 parameters computed from different starting structures are rather consistent in the ff99SB case. Overall, when calculating S^2 parameters over short time windows, an improved description of internal dynamics by ff99SB over ff99 becomes obvious.

Longer MD simulations should in principle help to overcome a lack of adequate sampling and result in a better description of the dynamics of mobile protein regions (5). As an attempt to further improve the agreement between computed and experimental S^2 values, we thus extended the trajectories of 1HEL to 100 ns simulation length. Assigning the loop 2 conformations again to one of the four clusters revealed no obvious change in the frequency of transitions between cluster 1 and 3 in the case of ff99 (Fig. S6 in Data S1). However, in the case of ff99SB, cluster 1 conformations almost exclusively prevail beyond a simulation time of 30 ns. The more restricted dynamics of the loop 2 region in the case of ff99SB compared to ff99 is also reflected in the S^2 parameters. If calculated from time windows of 1 ns and subsequent averaging, the thus-obtained S^2 parameters from the ff99SB trajectory agree well with those from 6LYT and 1IEE trajectories and show the best agreement with experiment (RMSD = 0.037). In contrast, ff99 simulation-derived S^2 parameters are still at variance with experiment (RMSD = 0.122).

Our results demonstrate that caution should be taken in general when simulated S^2 parameters are compared to experimental data with the aim of judging force-field quality. To assess the consistency of computed S^2 parameters, trajectories started from conformationally varying structures should be evaluated in parallel whenever possible. Adequately sampling flexible regions (~100 ns) with the aim to obtain an accurate representation of the structure and dynamics and only calculating S^2 parameters over short time windows (~1 ns) furthermore proved necessary to obtain consistent and accurate results irrespective of the starting coordinates.

SUPPLEMENTARY MATERIAL

To view all of the supplemental files associated with this article, visit www.biophysj.org.

ACKNOWLEDGMENTS

REFERENCES and FOOTNOTES

1. Case, D. A. 2002. Molecular dynamics and NMR spin relaxation in proteins. *Acc. Chem. Res.* 35:325–331.

2. Brüschweiler, R. 2003. New approaches to the dynamic interpretation and prediction of NMR relaxation data from proteins. *Curr. Opin. Struct. Biol.* 13:175–183.

3. Smith, L. J., A. E. Mark, C. M. Dobson, and W. F. van Gunsteren. 1995. Comparison of MD simulations and NMR experiments for hen lysozyme. Analysis of local fluctuations, cooperative motions, and global changes. *Biochemistry.* 34:10918–10931.

4. Lipari, G., and A. Szabo. 1982. Model-free approach to the interpretation of nuclear magnetic resonance relaxation in macromolecules. 1. Theory and range of validity. *J. Am. Chem. Soc.* 104:4546–4559.

5. Showalter, S. A., and R. Brüschweiler. 2007. Validation of molecular dynamics simulations of biomolecules using NMR spin relaxation as benchmarks: application to the AMBER99SB force field. *J. Chem. Theory Comput.* 3:961–975.

6. Hornak, V., R. Abel, A. Okur, B. Strockbine, A. Roitberg, and C. Simmerling. 2006. Comparison of multiple AMBER force fields and development of improved protein backbone parameters. *Proteins Struct. Funct. Bioinformat.* 65:712–725.

7. Buck, M., S. Bouguet-Bonnet, R. W. Pastor, and A. D. MacKerell. 2006. Importance of the CMAP correction to the CHARMM22 protein force field: dynamics of hen lysozyme. *Biophys. J.* 90:L36–L38.

8. Soares, T., X. Daura, C. Oostenbrink, L. Smith, and W. F. van Gunsteren. 2004. Validation of the GROMOS force-field parameter set 45A3 against nuclear magnetic resonance data of hen egg lysozyme. *J. Biomol. NMR.* 30:407–422.

9. Clore, G. M., A. Szabo, A. Bax, L. E. Kay, P. C. Driscoll, and A. M. Gronenborn. 1990. Deviations from the simple two-parameter model-free approach to the interpretation of nitrogen-15 nuclear magnetic relaxation of proteins. *J. Am. Chem. Soc.* 112:4989–4991.

10. Horita, D. A., W. Zhang, T. E. Smithgall, W. H. Gmeiner, and R. A. Byrd. 2000. Dynamics of the Hck-SH3 domain: comparison of experiment with multiple molecular dynamics simulations. *Protein Sci.* 9:95–103.

11. Andrews, B. K., T. Romo, J. B. Clarage, B. M. Pettitt, and G. N. Phillips. 1998. Characterizing global substates of myoglobin. *Structure.* 6:587–594.

12. Halle, B. 2002. Flexibility and packing in proteins. *Proc. Natl. Acad. Sci. USA.* 99:1274–1279.

13. Stocker, U., and W. F. van Gunsteren. 2000. Molecular dynamics simulation of hen egg white lysozyme: a test of the GROMOS96 force field against nuclear magnetic resonance data. *Proteins.* 40:145–153.

14. Schwalbe, H., S. B. Grimshaw, A. Spencer, M. Buck, J. Boyd, C. M. Dobson, C. Redfield, and L. J. Smith. 2001. A refined solution structure of hen lysozyme determined using residual dipolar coupling data. *Protein Sci.* 10:677–688.

15. Case, D. A., T. Cheatham, T. Darden, H. Gohlke, R. Luo, K. M. Merz, A. Onufriev, C. Simmerling, B. Wang, and R. Woods. 2005. The AMBER biomolecular simulation programs. *J. Comput. Chem.* 26:1668–1688.

16. Wang, J., P. Cieplak, and P. Kollman. 2000. How well does a restrained electrostatic potential (RESP) model perform in calculating conformational energies of organic and biological molecules? *J. Comput. Chem.* 21:1049–1074.

17. Prompers, J. J., and R. Brüschweiler. 2002. General framework for studying the dynamics of folded and nonfolded proteins by NMR relaxation spectroscopy and MD simulation. *J. Am. Chem. Soc.* 124:4522–4534.

18. Buck, M., J. Boyd, C. Redfield, D. A. MacKenzie, D. J. Jeenes, D. B. Archer, and C. M. Dobson. 1995. Structural determinants of protein dynamics: analysis of ^{15}N NMR relaxation measurements for main-chain and side-chain nuclei of hen egg white lysozyme. *Biochemistry.* 34:4041–4055.

19. Nederveen, A. J., and A. Bonvin. 2005. NMR relaxation and internal dynamics of ubiquitin from a 0.2 microsec MD simulation. *J. Chem. Theory Comput.* 1:363–374.